Electronic Supplementary Information

Blue and white-light emitting 2D-coordination polymers and their solid-state photochemical [2+2] cycloaddition reaction

Abdul Malik P. Peedikakkal[a,c]*, Almaz S. Jalilov[a,d], Abdul Rajjak Shaikh[b], Abdul Nasar Kalanthoden[a], Abdulaziz A. Al-Saadi[a,e]

[a] *Department of Chemistry, King Fahd University of Petroleum and Minerals, P.O. Box 1710, Dhahran 31261, Saudi Arabia*

[b] *KAUST Catalysis Center (KCC), Physical Sciences and Engineering Division (PSE), King Abdullah University of Science and Technology (KAUST), Thuwal, 23955-6900, Saudi Arabia*

[c]*Interdisciplinary Research Center for Hydrogen and Energy Storage, King Fahd University of Petroleum and Minerals, Dhahran 31261, Saudi Arabia*

[d]*Interdisciplinary Research Center for Advanced Materials, King Fahd University of Petroleum and Minerals, Dhahran 31261, Saudi Arabia*

[e]*Interdisciplinary Research Center for Refining and Advanced Chemicals, King Fahd University of Petroleum and Minerals, Dhahran 31261, Saudi Arabia*

Table of Contents

X-ray Crystallography

.

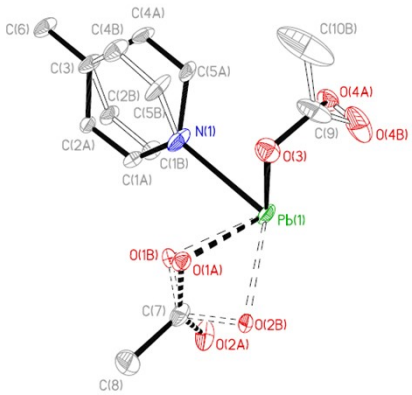

Figure S1. Thermal ellipsoid (20%) plot of asymmetric unit of **1**. Fluorine atoms and one of the oxygen atoms (O3 and O3A) in CH_3CO_2 are disordered

.

*Table S1***.** Selected bond lengths (Å) and bond angles (°) in **1**

Pb(1)-O(1B)	2.317(14)	O(1B)-Pb(1)-O(2B)#1	89.2(5)
Pb(1)-O(3)	2.382(8)	O(3)-Pb(1)-O(2B)#1	75.1(4)
Pb(1)-N(1)	2.551(9)	N(1)-Pb(1)-O(2B)#1	148.2(5)
Pb(1)-O(1A)	2.588(13)	O(1A)-Pb(1)-O(2B)#1	70.1(5)
Pb(1)-O(2B)#1	2.700(14)	O(1B)-Pb(1)-O(2B)	51.6(5)
Pb(1)-O(2B)	2.703(16)	O(3)-Pb(1)-O(2B)	87.5(4)
Pb(1)-O(4A)	2.79(3)	N(1)-Pb(1)-O(2B)	120.6(4)

Pb(1)-O(4B)	2.81(7)	O(1A)-Pb(1)-O(2B)	39.6(4)
Pb(1)-O(2A)	2.89(0)	O(2B)#1-Pb(1)-O(2B)	39.4(6)
Pb(1)-O(2A)#1	2.86(9)	C(9)-O(3)-Pb(1)	102.5(10)
Pb(1)-O(3)#1	2.82(1)	C(7)-O(1A)-Pb(1)	98.6(9)
O(2B)-Pb(1)#1	2.700(14)	C(7)-O(1B)-Pb(1)	108.1(10)
O(1B)-Pb(1)-O(3)	88.8(5)	C(7)-O(2B)-Pb(1)#1	127.6(11)
O(1B)-Pb(1)-N(1)	70.0(5)	O(2B)#1-O(2B)-Pb(1)#1	70.4(6)
O(3)-Pb(1)-N(1)	80.4(3)	C(7)-O(2B)-Pb(1)	88.4(9)
O(1B)-Pb(1)-O(1A)	24.8(5)	O(2B)#1-O(2B)-Pb(1)	70.2(6)
O(3)-Pb(1)-O(1A)	69.2(4)	Pb(1)#1-O(2B)-Pb(1)	93.4(5)
N(1)-Pb(1)-O(1A)	82.4(4)		
Symmetry transformations used to generate equivalent atoms: #1 -x,y,-z+3/2 #2 -x+1,-y,-z+1			

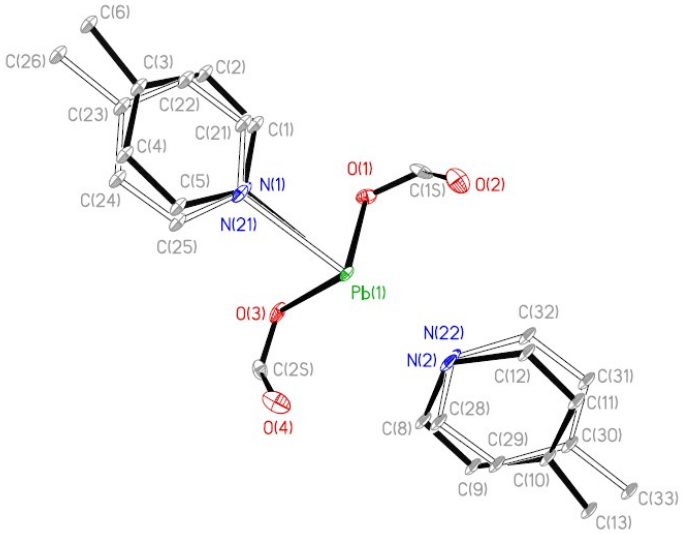

Figure S2. Thermal ellipsoid (20%) plot of asymmetric unit of **2**.

.

*Table S2***.** Selected bond lengths (Å) and bond angles (°) in **2**

Pb(1)-O(3)	2.384(8)	O(3)-Pb(1)-N(21)	78.0(7)
Pb(1)-O(1)	2.420(8)	O(1)-Pb(1)-N(21)	79.0(7)
Pb(1)-O(2)	2.892(0)	N(1)-Pb(1)-N(21)	2.5(13)
Pb(1)-O(4)	2.884(6)	C(1)-N(1)-Pb(1)	117.1(12)
Pb(1)-N(1)	2.551(13)	C(5)-N(1)-Pb(1)	122.3(12)
Pb(1)-N(21)	2.563(13)	C(21)-N(21)-Pb(1)	123.1(12)
O(3)-Pb(1) -O(1)	76.7(3)	C(25)-N(21)-Pb(1)	116.1(12)
O(3)-Pb(1) -N(1)	76.7(3)	C(1S)-O(1)-Pb(1)	104.2(8)
O(1)-Pb(1) -N(1)	76.6(7)	C(2S)-O(3)-Pb(1)	105.0(8)
Symmetry transformations used to generate equivalent atoms: #1 -x,y,-z+3/2 #2 -x+1,-y,-z+1			

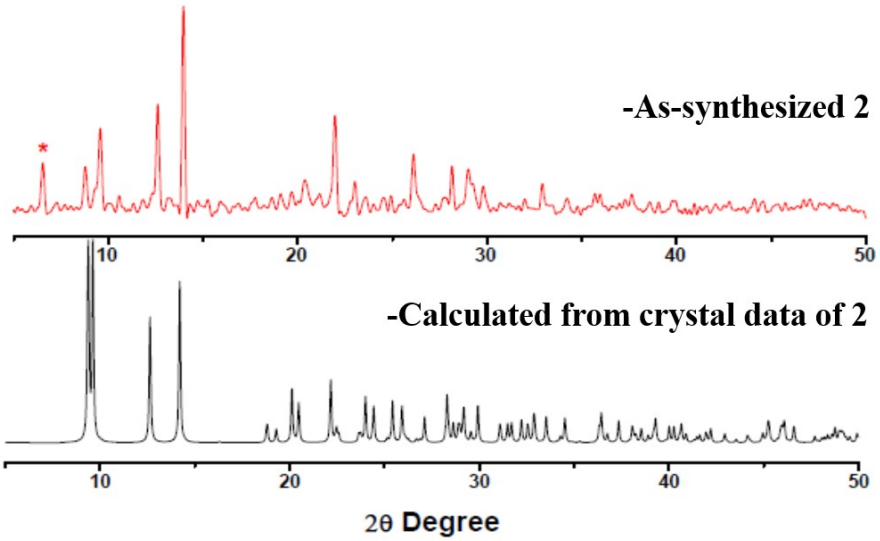

Figure S3. Experimental and calculated PXRD patterns for compound **2**.

.

NMR spectra

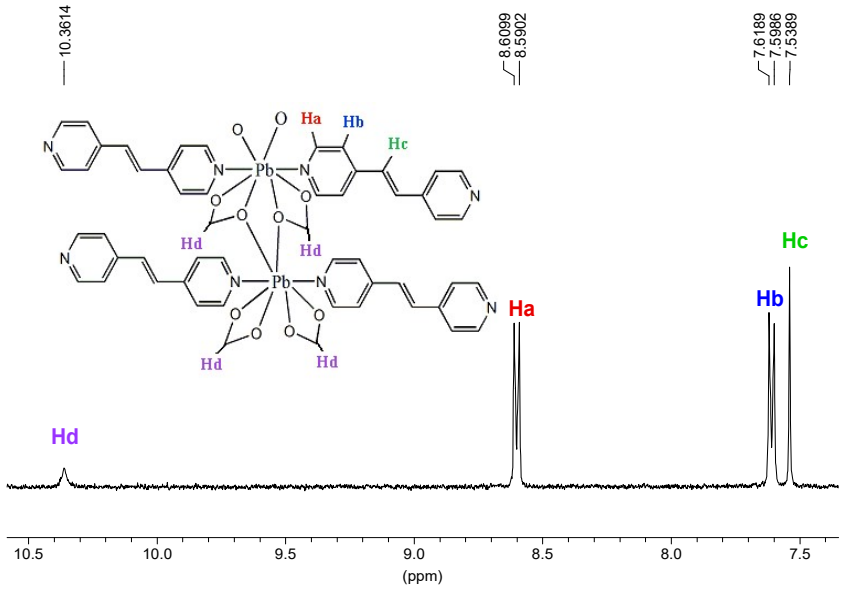

Figure S4. ^{1}H NMR spectrum of **2** (DMSO-d_6, 300 MHz, 298K) before UV irradiation.

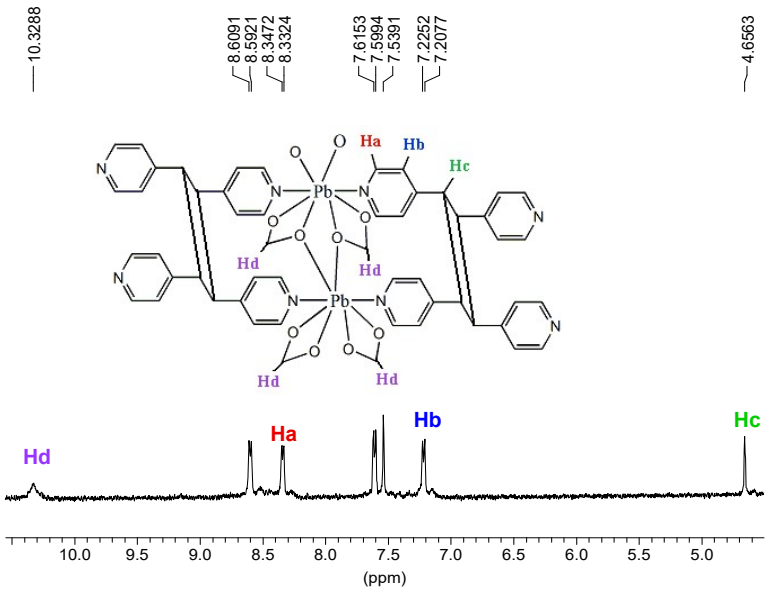

Figure S5. ^{1}H NMR spectrum (DMSO-d_6, 300 MHz, 298K) of **2,** ground crystal after 3 hr irradiation.The percentage of photo conversion is 67% of *rctt*-tpcb and 33% of bpe.

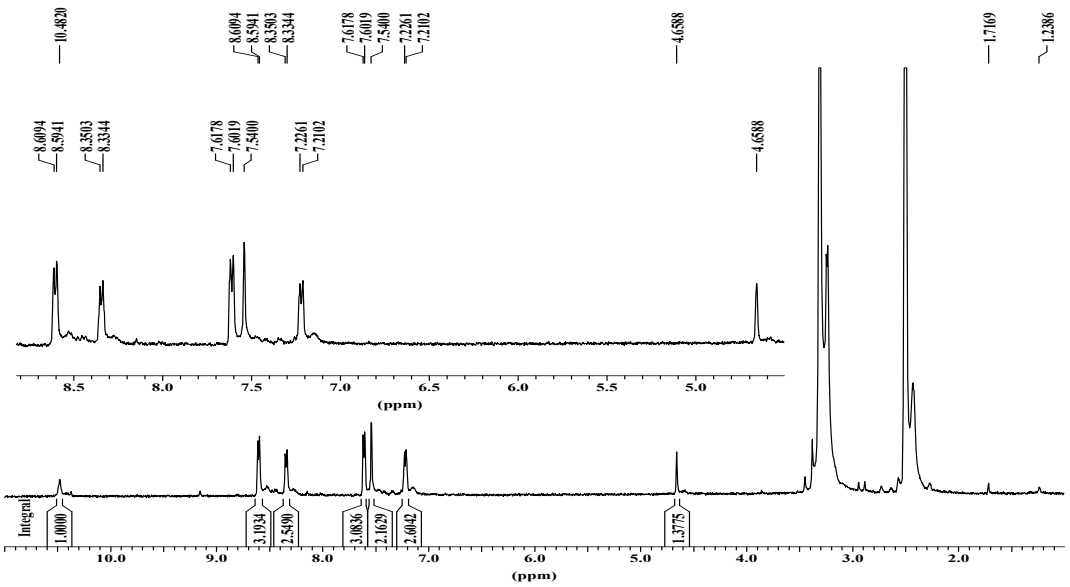

Figure S6. [1]H NMR spectrum of **2** after 1 h UV irradiation

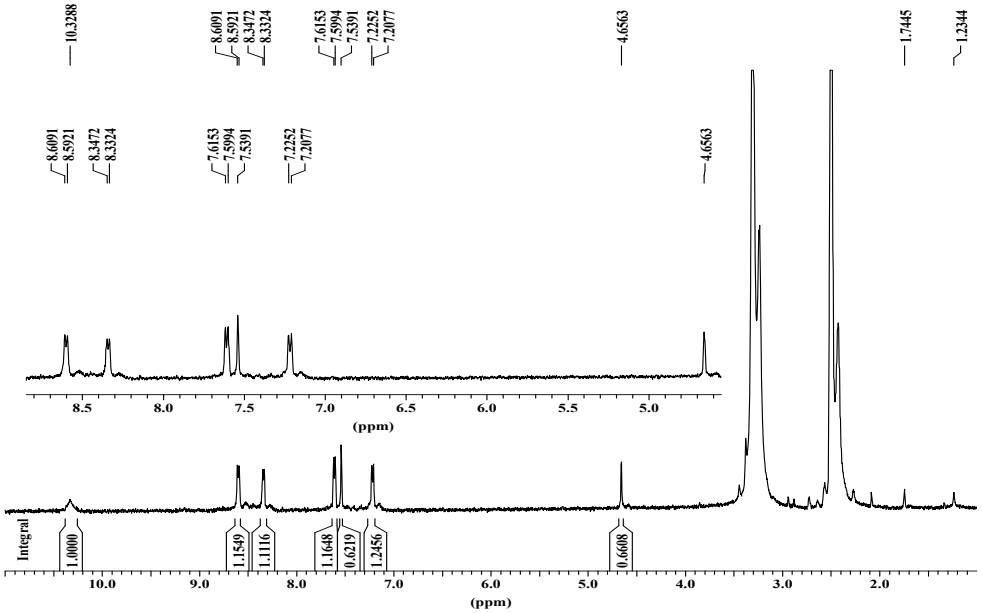

Figure S7. [1]H NMR spectrum of **2** after 3 h UV irradiation.

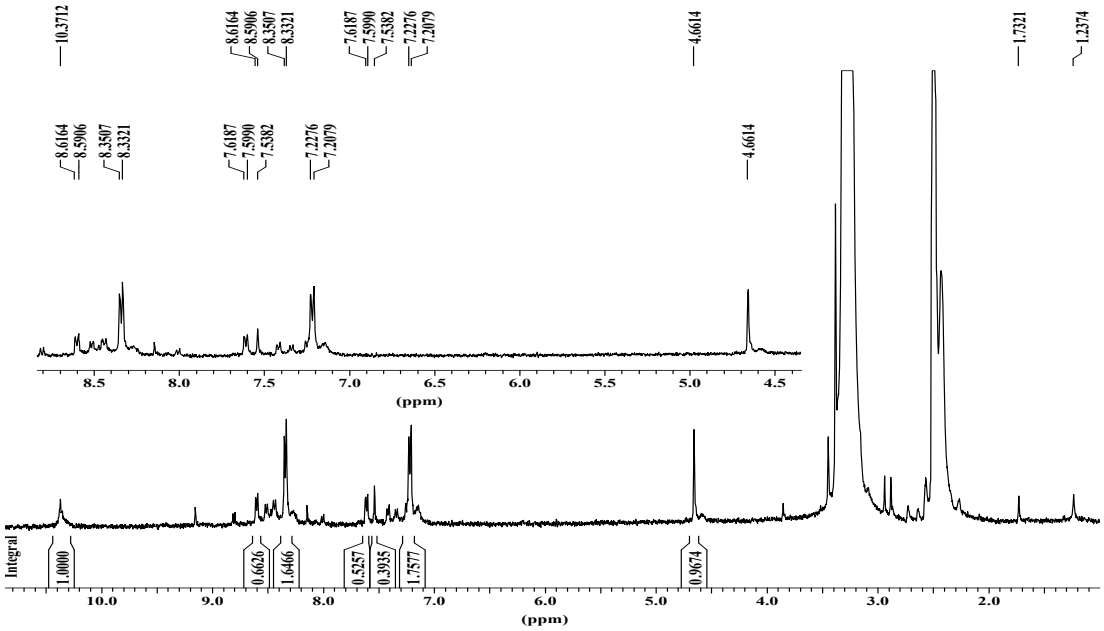

Figure S8. ^{1}H NMR spectrum of **2** after 15 h UV irradiation.

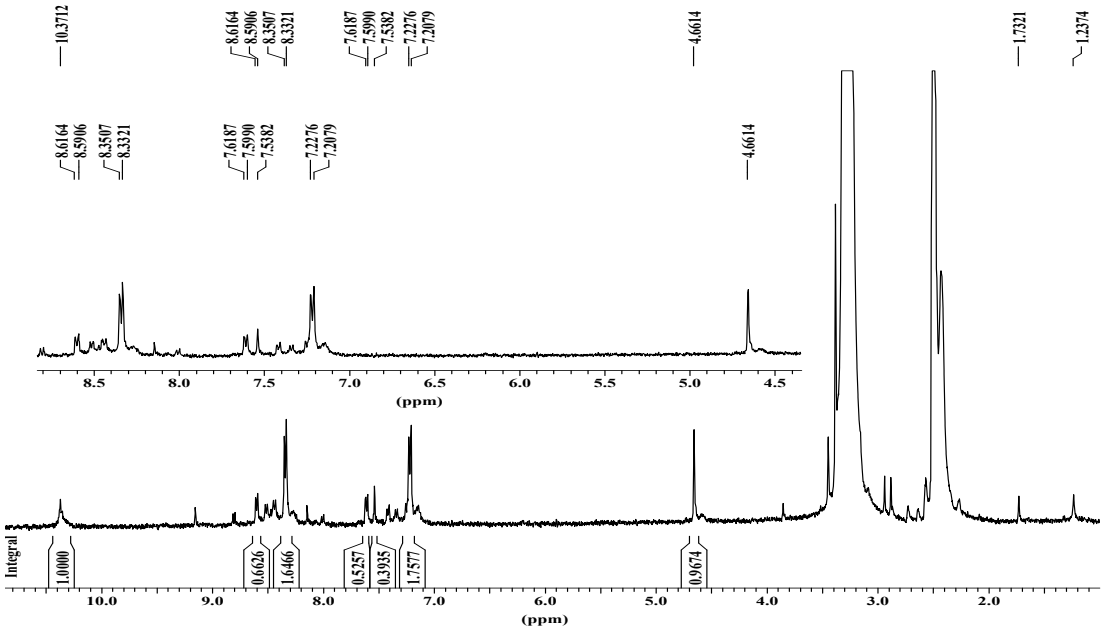

Figure S9. ^{1}H NMR spectrum of **2** after 36 h UV irradiation.

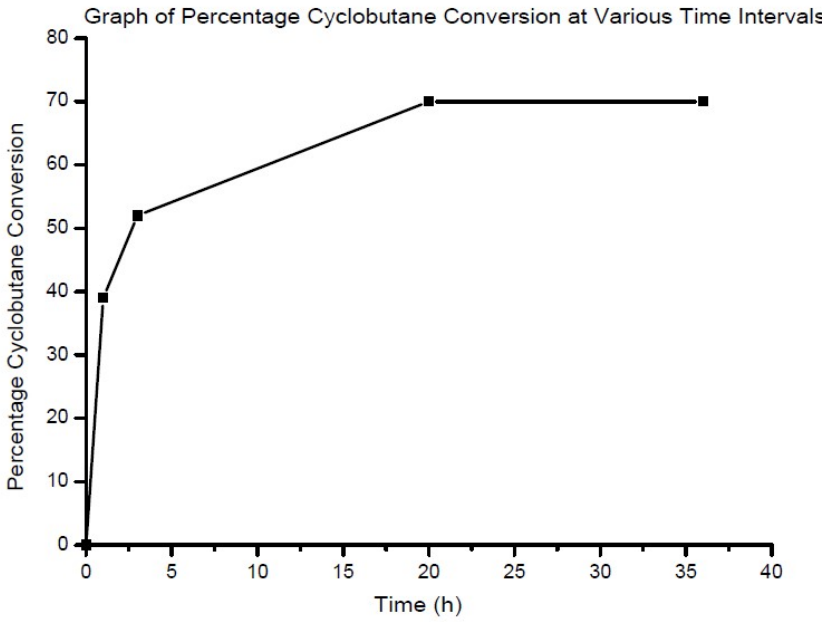

Figure S10. Plots of the product formed versus time for ground single crystal of **2**.

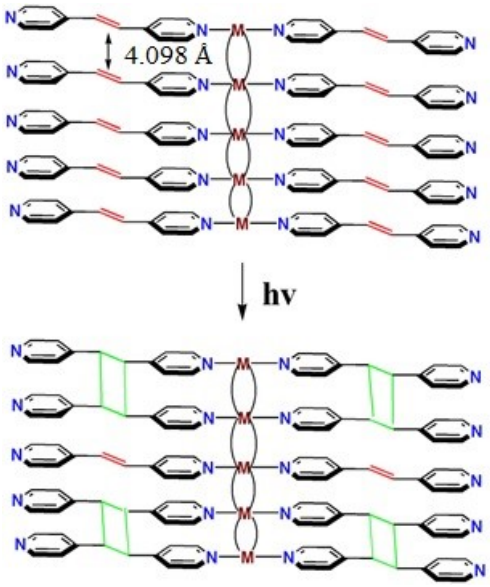

Scheme S1. Schematic diagram representing the possible photoreaction pathways of **2** in one step (67% *rctt-tpcb* dimer). It is not possible to produces 100% photodimer if the cycloaddition takes place in this pathway.

FT-IR Spectra

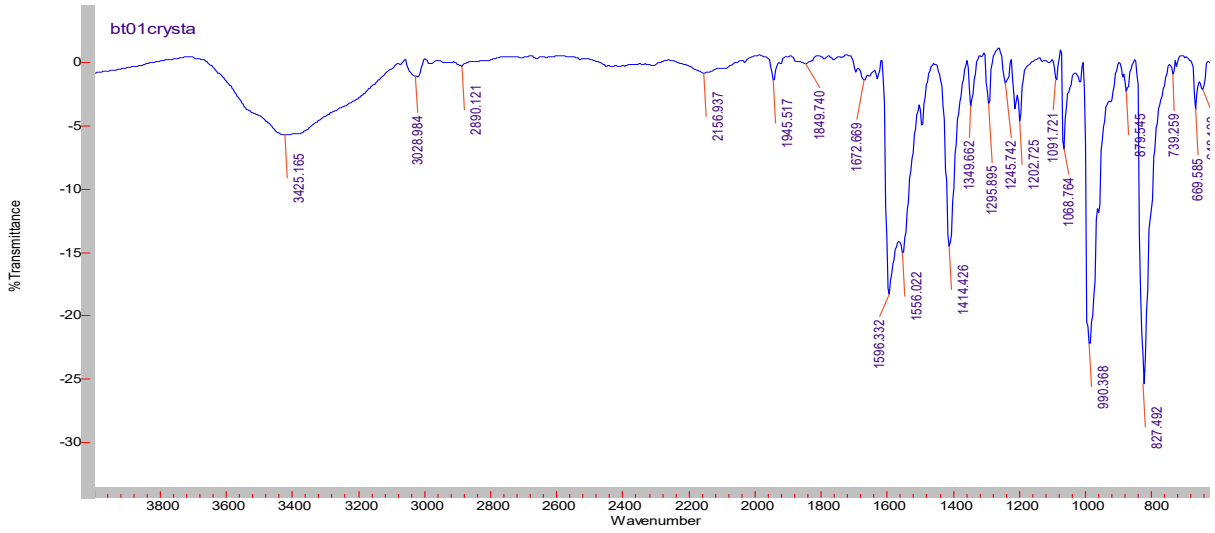

Figure S11. FT-IR Spectra of **1**

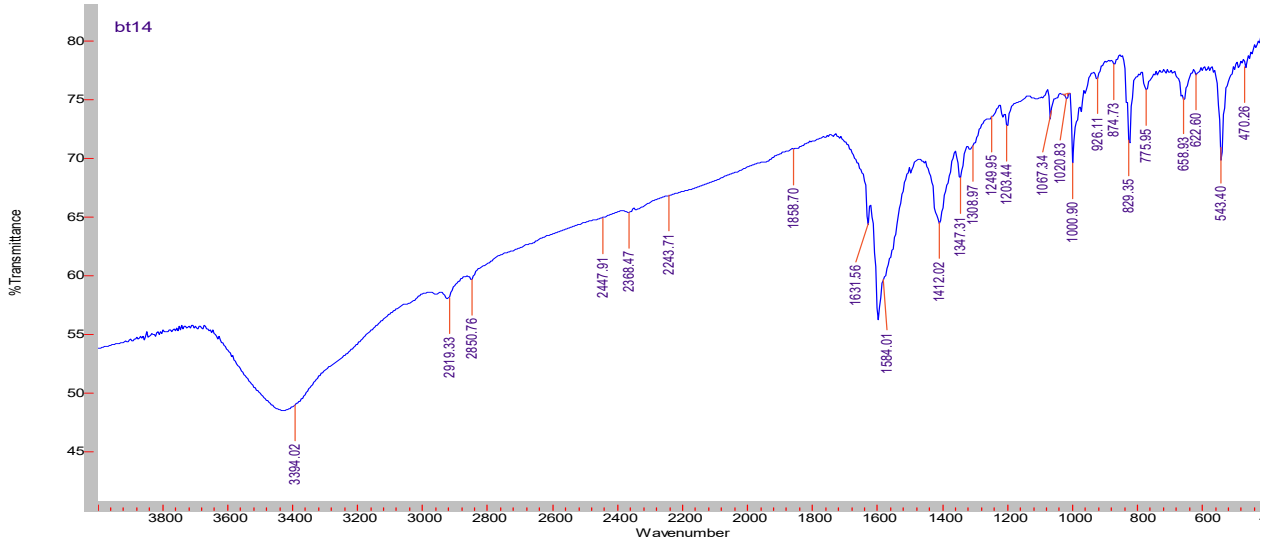

Figure S12. FT-IR Spectra of **2**

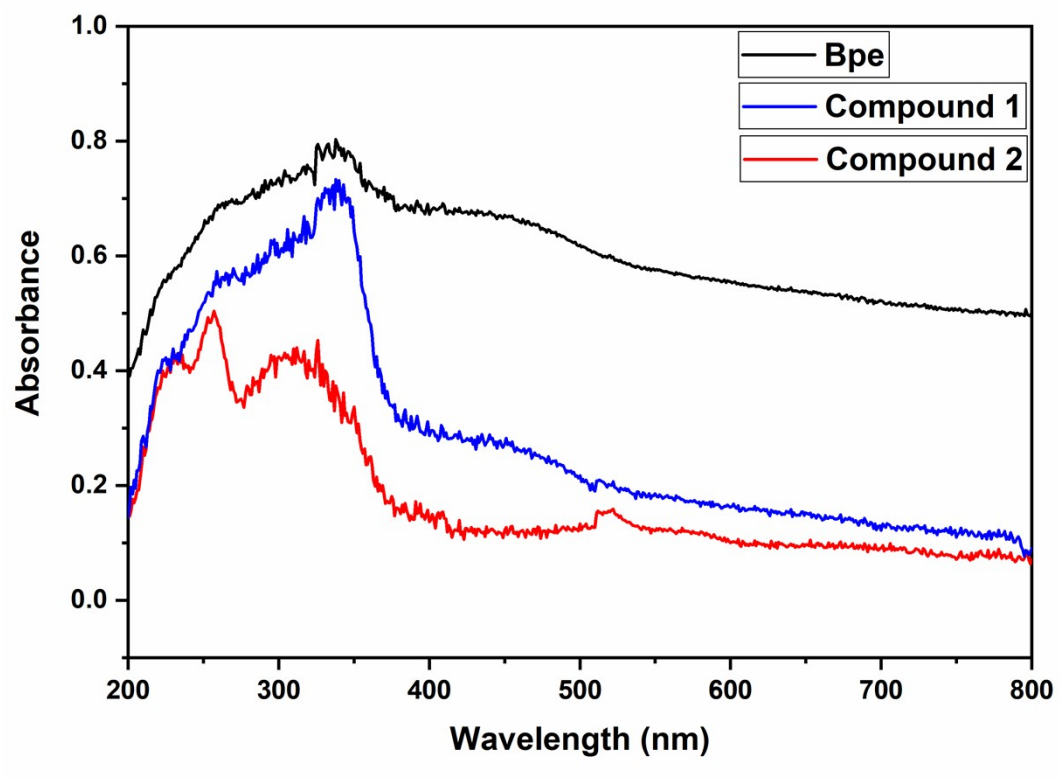

Figure S13. Solid-state UV/Vis spectra of compounds, bpe and **1**-**2**.

Computational Methods:

Quantum chemical density functional theory (DFT) calculations were carried out using the B3LYP hybrid functional implemented in the Gaussian-16 suite of programs.[1] The molecular structures of studied complex was optimized starting from the structural data obtained during the XRD measurements. The metal (Pb) atoms were described by the LANL2DZ basis set, while the 6-31G(d,p) basis set was applied for C, H, N, O. Same method was previously utilized and found to be in good agreement with experiment.[2] Optimized geometry was evaluated through calculation of the vibrational frequencies with the absence of any imaginary value, what corresponds to the states with minimum energy. Time dependent DFT calculations with the B3LYP functional were applied to obtain absorption spectra. The Avogadro[3] 1.2.0 and GaussSum[4] 3.0 programs were used for visualization of the molecular orbitals and extraction of the percent contributions of groups of atoms to each of the MOs, respectively.

Computational Results:

Quantum chemical computations elucidate further insight into the photophysical properties of the coordination polymers. We have selected [Pb(μ-bpe)(μ-$O_2CCH_3)_2$] and [Pb(μ-bpe)(μ-$O_2CH)_2$] as a system to mimic the major contribution of the photophysical properties of the compound **1** and **2**, which show features of the MC transitions (Figure S14 and Figure S15) as the component of the white-light emitting and blue emission photoluminescence in **1** and **2** .

*Table S3***.** Orbital energies for the **1** and **2**.

Orbital	Energy (eV)	
	1	**2**
HOMO	-6.345	-6.865
LUMO	-2.047	-2.528
HOMO-1	-6.392	-6.992
LUMO+1	-1.778	-2.266
HOMO-2	-6.489	-7.099
LUMO+2	-1.301	-1.595
HOME-3	-6.57	-7.111
LUMO+3	-1.258	-1.533
HOME-4	-6.873	-7.317
LUMO+4	-0.681	-0.941

References:

1. Frisch, M. J.; Trucks, G. W.; Schlegel, H. B.; Scuseria, G. E.; Robb, M. A.; Cheeseman, J. R.; Scalmani, G.; Barone, V.; Mennucci, B.; Petersson, G. A. et al., Gaussian 16, Revision B.01. Wallingford CT, 2016.
2. A. M. P. Peedikakkal, H. S. Quah, S. Chia, A. S. Jalilov, A. R. Shaikh, H. A. Al-Mohsin, K. Yadava, W. Ji and J. J. Vittal, *Inorg. Chem.*, 2018, **57**, 11341–11348.
3. Hanwell, M. D.; Curtis, D. E.; Lonie, D. C.; Vandermeersch, T.; Zurek, E.; Hutchison, G. R. J. Cheminform. 2012, **4**, 17.
4. O'Boyle, N. M.; Tenderholt, A. L.; Langner, K. M. *J. Comp. Chem.*, 2008, **29**, 839.

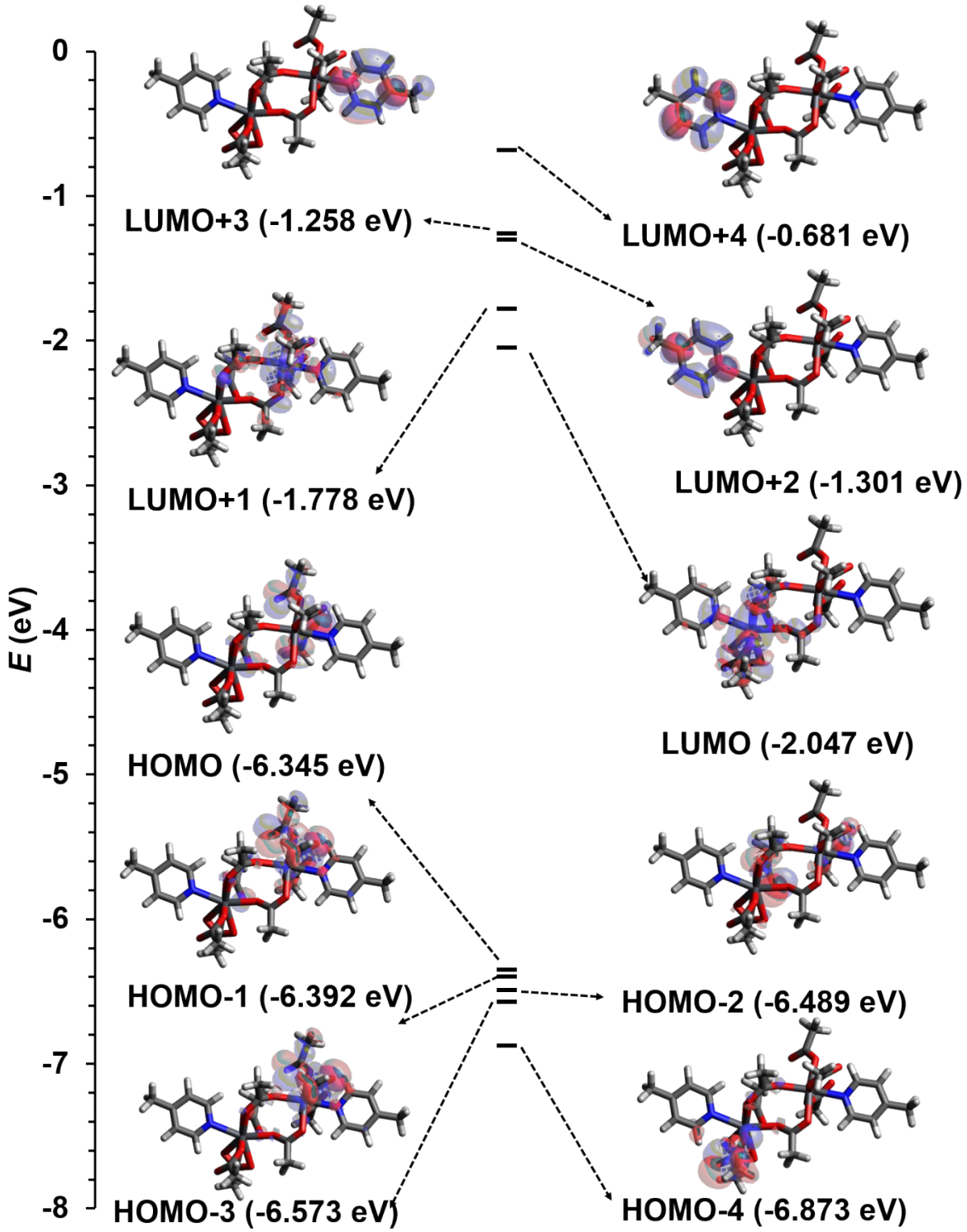

Figure S14. Energy levels of the lower energy transitions and the frontier orbitals for the compound **1**.

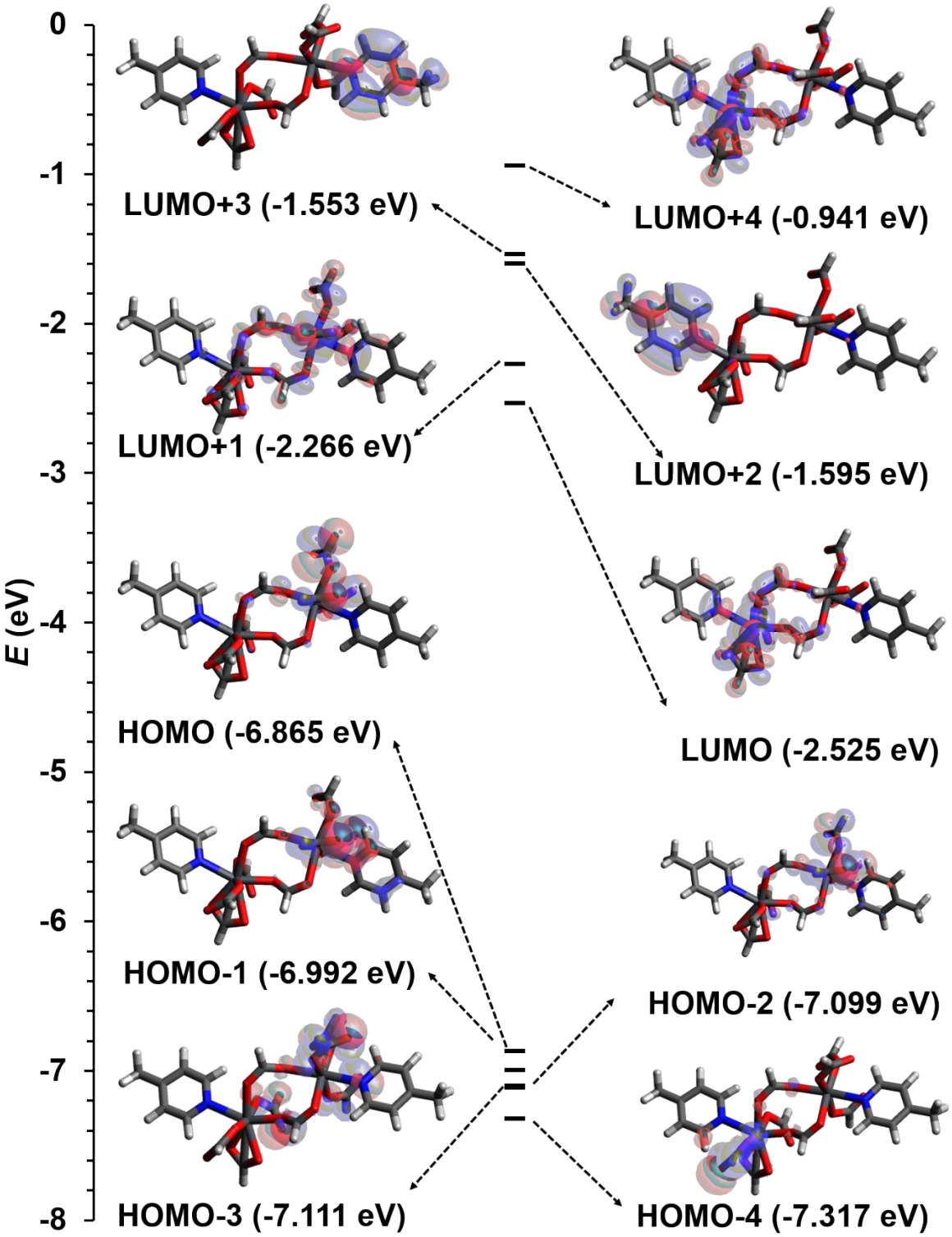

Figure S15. Energy levels of the lower energy transitions and the frontier orbitals for the compound **2**.

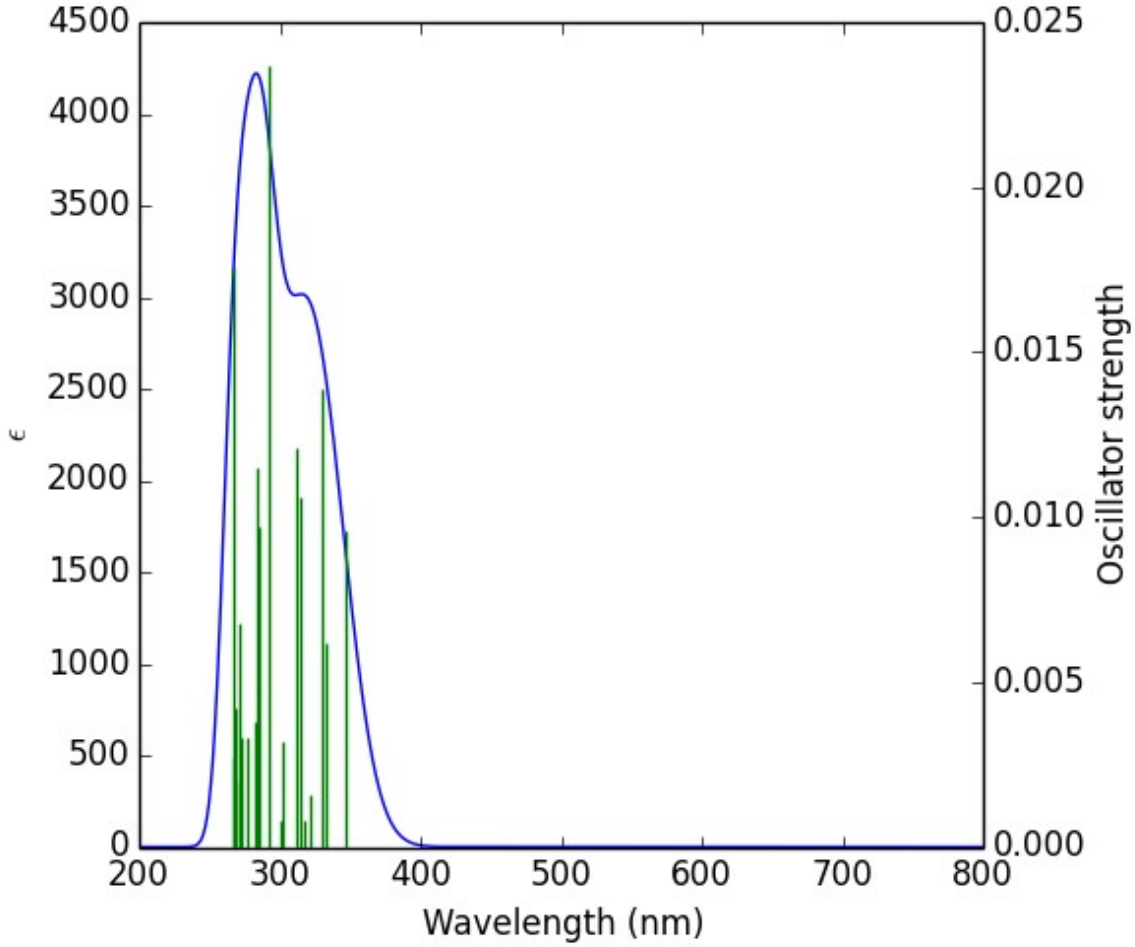

Figure S16. UV-Vis spectrum of compound **1** calculated (blue) and calculated using TD-DFT (green).

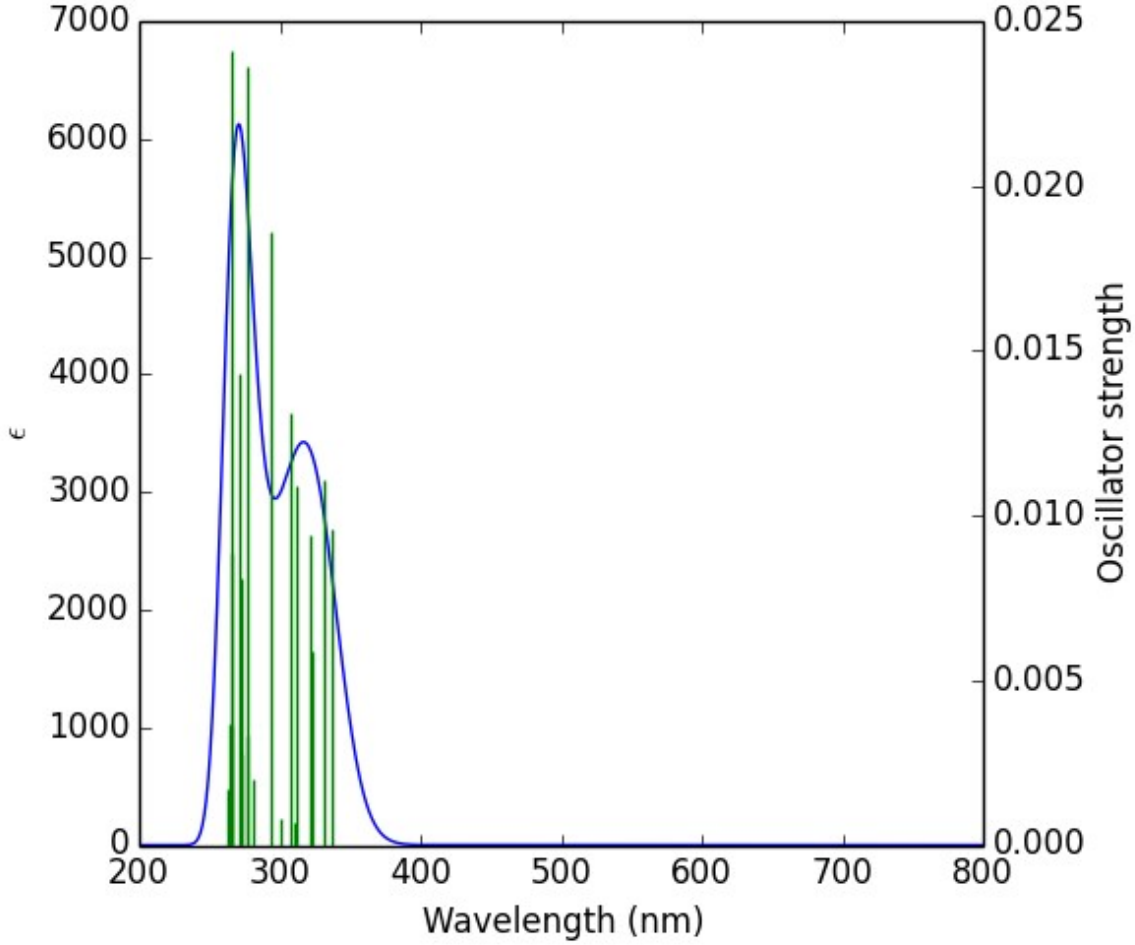

Figure S17. UV-Vis spectrum of compound **2** calculated (blue) and calculated using TD-DFT (green).

Table S4: The highest wavelength absorption data from calculations (TD-DFT) for the studied compound **1.**

Calculated Wavelength (nm)	Oscillator Strength	Major contributions
347.4188	0.0096	H-2(A)->LUMO(A) (40%), H-2(B)->LUMO(B) (40%)
333.2975	0.0062	HOMO(A)->L+1(A) (45%), HOMO(B)->L+1(B) (45%)
329.5151	0.0139	H-1(A)->L+1(A) (45%), H-1(B)->L+1(B) (45%)
321.7254	0.0016	HOMO(A)->LUMO(A) (38%), HOMO(B)->LUMO(B) (38%)
317.2309	0.0008	H-1(A)->LUMO(A) (35%), H-1(B)->LUMO(B) (35%)
314.3992	0.0106	H-3(A)->L+1(A) (46%), H-3(B)->L+1(B) (46%)
312.3872	0.0121	H-4(A)->LUMO(A) (48%), H-4(B)->LUMO(B) (48%)
302.1773	0.0032	H-3(A)->LUMO(A) (42%), H-3(B)->LUMO(B) (42%)
300.3327	0.0008	H-2(A)->L+1(A) (45%), H-2(B)->L+1(B) (45%)
292.021	0.0237	H-7(A)->LUMO(A) (21%), H-5(A)->LUMO(A) (21%), H-7(B)->LUMO(B) (21%), H-5(B)->LUMO(B) (21%)
285.2487	0.0097	H-6(A)->LUMO(A) (12%), H-5(A)->LUMO(A) (21%), H-6(B)->LUMO(B) (12%), H-5(B)->LUMO(B) (21%)
283.3063	0.0115	H-5(A)->L+1(A) (44%), H-5(B)->L+1(B) (44%)
282.6733	0	H-9(A)->L+1(A) (25%), H-9(B)->L+1(B) (25%)
282.4608	0.0038	HOMO(A)->L+3(A) (42%), HOMO(B)->L+3(B) (42%)
276.4277	0.0033	H-3(A)->L+3(A) (11%), H-1(A)->L+3(A) (34%), H-3(B)->L+3(B) (11%), H-1(B)->L+3(B) (34%)
273.1392	0.0033	H-6(A)->L+1(A) (28%), H-6(B)->L+1(B) (28%)
271.8158	0.0068	H-15(A)->LUMO(A) (17%), H-15(B)->LUMO(B) (17%)
269.0669	0.002	H-9(A)->L+1(A) (23%), H-9(B)->L+1(B) (23%)
268.8452	0.0042	H-12(A)->LUMO(A) (15%), H-10(A)->LUMO(A) (12%), H-12(B)->LUMO(B) (15%), H-10(B)->LUMO(B) (12%)
267.3495	0.0027	H-2(A)->L+2(A) (29%), HOMO(A)->L+2(A) (12%), H-2(B)->L+2(B) (29%), HOMO(B)->L+2(B) (12%)
267.0098	0.0176	H-14(A)->LUMO(A) (12%), H-6(A)->LUMO(A) (10%), H-14(B)->LUMO(B) (12%), H-6(B)->LUMO(B) (10%)

Table S5: The highest wavelength absorption data from calculations (TD-DFT) for the studied compound **2.**

Calculated Wavelength (nm)	Oscillatory Strength	Major contributions
329.8482	0.0148	H-3(A)->LUMO(A) (41%), H-3(B)->LUMO(B) (41%)
328.2588	0.013	HOMO(A)->LUMO(A) (10%), HOMO(A)->L+1(A) (33%), HOMO(B)->LUMO(B) (10%), HOMO(B)->L+1(B) (33%)
320.0479	0.025	H-1(A)->L+1(A) (39%), H-1(B)->L+1(B) (39%)
315.5194	0.0022	HOMO(A)->LUMO(A) (34%), HOMO(A)->L+1(A) (13%), HOMO(B)->LUMO(B) (34%), HOMO(B)->L+1(B) (13%)
312.4344	0.0244	H-4(A)->LUMO(A) (26%), H-2(A)->L+1(A) (15%), H-4(B)->LUMO(B) (26%), H-2(B)->L+1(B) (15%)
311.1719	0.0084	H-4(A)->LUMO(A) (20%), H-2(A)->L+1(A) (21%), H-4(B)->LUMO(B) (20%), H-2(B)->L+1(B) (21%)
304.6124	0.0014	H-1(A)->LUMO(A) (39%), H-1(B)->LUMO(B) (39%)
299.361	0.0012	H-2(A)->LUMO(A) (31%), H-2(A)->L+1(A) (12%), H-2(B)->LUMO(B) (31%), H-2(B)->L+1(B) (12%)
291.8422	0.0225	H-5(A)->LUMO(A) (18%), H-3(A)->L+1(A) (17%), H-5(B)->LUMO(B) (18%), H-3(B)->L+1(B) (17%)
287.4576	0.0347	H-5(A)->LUMO(A) (12%), H-3(A)->L+1(A) (12%), H-5(B)->LUMO(B)

		(12%), H-3(B)->L+1(B) (12%)
286.0384	0.0044	H-5(A)->LUMO(A) (10%), H-5(B)->LUMO(B) (10%)
279.9795	0.0018	H-8(A)->L+1(A) (10%), H-5(A)->L+1(A) (19%), H-8(B)->L+1(B) (10%), H-5(B)->L+1(B) (19%)
278.8335	0.0056	H-15(A)->LUMO(A) (15%), H-9(A)->LUMO(A) (11%), H-15(B)->LUMO(B) (15%), H-9(B)->LUMO(B) (11%)
275.5859	0.007	H-8(A)->L+1(A) (14%), H-5(A)->L+1(A) (10%), H-8(B)->L+1(B) (14%), H-5(B)->L+1(B) (10%)
274.3723	0.0006	H-7(A)->LUMO(A) (16%), H-7(B)->LUMO(B) (16%)
271.4765	0.0023	H-10(A)->L+1(A) (22%), H-10(B)->L+1(B) (22%)
270.5406	0.007	H-11(A)->L+1(A) (15%), H-11(B)->L+1(B) (15%)
268.5075	0.0011	H-4(A)->L+1(A) (43%), H-4(B)->L+1(B) (43%)
266.9408	0.0147	H-14(A)->LUMO(A) (13%), H-14(B)->LUMO(B) (13%)
265.0519	0.0023	H-17(A)->LUMO(A) (16%), H-16(A)->LUMO(A) (12%), H-17(B)->LUMO(B) (16%), H-16(B)->LUMO(B) (12%)
264.8481	0.0039	HOMO(A)->L+3(A) (36%), HOMO(B)->L+3(B) (36%)

Table S6: Coordinates for the B3LYP/LANL2DZ/6-31G(d,p) -optimized structure of the Compound **1**. Energy: -2410.14962123 au

86

C	6.86050	1.95240	-0.06030
C	-6.48620	-2.74310	-0.19210
C	8.19850	2.64320	0.00170
C	0.39280	1.82090	-0.84740
C	2.68270	0.36470	2.62100
C	-0.54540	-1.65020	-1.20150
C	-1.44650	-0.16460	2.69060
C	-0.02970	3.10730	-1.51540
C	2.16030	1.17430	3.79680
C	-0.32510	-2.71910	-2.25270
C	-0.94680	-1.23910	3.63340
C	3.59450	-1.37350	-2.81790
C	2.81240	-2.92250	1.42400
C	-3.86060	2.07160	-2.19510
C	-3.60010	2.62550	1.38800
C	3.39120	-1.66220	-4.29930
C	3.73420	-4.05280	1.84530
C	-3.72410	2.68810	-3.57870
C	-4.15720	3.74610	2.22260
C	4.48310	1.96100	-0.48080
C	-4.13690	-2.24310	0.06290
C	5.69470	2.63910	-0.41770
C	-5.17320	-3.16710	0.05200
C	6.73490	0.58640	0.22220
C	-6.67970	-1.37610	-0.41670
C	5.49570	-0.03130	0.13800
C	-5.59710	-0.50310	-0.38700
N	4.38810	0.64850	-0.21060
N	-4.34430	-0.93260	-0.15860
O	2.47350	-0.95120	-2.24190
O	3.28620	-2.25780	0.37120
O	-2.82260	1.31920	-1.87550
O	-4.11230	1.46290	1.44460
O	1.58900	1.41330	-1.05430
O	1.86630	0.43780	1.57480
O	-1.67490	-1.07470	-1.19830
O	-1.98160	-0.68270	1.58700

O	-0.40110	1.17270	-0.12090
O	3.74530	-0.23820	2.64090
O	0.38290	-1.42790	-0.36340
O	-1.35630	1.03550	2.90060
O	4.66790	-1.52280	-2.25960
O	1.77270	-2.65750	2.00170
O	-4.83530	2.27330	-1.48180
O	-2.58420	2.81080	0.64970
Pb	2.32710	-0.50690	-0.20210
Pb	-2.50890	0.60910	0.07350
H	8.08990	3.73180	0.01170
H	0.83100	3.64650	-1.91370
H	-0.58450	3.72030	-0.80040
H	-0.71460	2.85610	-2.33200
H	2.55560	2.19490	3.72000
H	2.52750	0.73680	4.72820
H	1.06970	1.23240	3.78630
H	-1.21260	-2.85640	-2.87210
H	0.52870	-2.42140	-2.86820
H	-0.05860	-3.65900	-1.75780
H	-1.70180	-2.02140	3.75710
H	-0.05470	-1.70230	3.19680
H	-0.70300	-0.79710	4.60130
H	2.70300	-2.50600	-4.42330
H	2.94160	-0.79780	-4.79790
H	4.34950	-1.90700	-4.76070
H	4.11840	-4.59190	0.97510
H	4.58980	-3.62090	2.37740
H	3.20440	-4.73180	2.51590
H	-4.68150	3.10860	-3.89100
H	-2.97590	3.48870	-3.54660
H	-3.37950	1.94280	-4.30110
H	-3.96120	4.70980	1.74920
H	-5.22710	3.60570	2.38650
H	-3.64820	3.72320	3.19320
H	3.55960	2.45560	-0.75590
H	-3.11410	-2.53640	0.25910
H	5.72270	3.70050	-0.64530
H	-4.95270	-4.21470	0.23550
H	7.60050	-0.00210	0.51090
H	-7.67200	-0.98140	-0.61410
H	5.35980	-1.08440	0.34300
H	-5.70950	0.56210	-0.55780
C	-7.63870	-3.71440	-0.18390
H	-8.48750	-3.33480	-0.76060
H	-7.34580	-4.68570	-0.59570
H	-7.98750	-3.88730	0.84260
H	8.75790	2.34320	0.89430
H	8.81030	2.37590	-0.86940

Table S7: Coordinates for the B3LYP/LANL2DZ/6-31G(d,p) -optimized structure of the Compound **2.** Energy: - =-2095.5836615 au
62

C	-6.89179	-1.67855	-0.32195
C	6.75061	2.12888	-0.45515
C	-8.23403	-2.35947	-0.36493
C	-0.42951	-1.75149	-0.20662
C	-3.27883	0.45118	2.73039

C	0.55398	1.76421	-0.56884
C	2.20443	-0.54403	3.05741
C	-2.58648	0.94525	-3.05828
C	-3.21545	3.42047	0.67478
C	2.97166	-1.84025	-2.57982
C	3.48804	-3.18943	0.65044
C	-4.52285	-1.69409	0.13973
C	4.46945	1.84186	0.28477
C	-5.74799	-2.34479	0.13607
C	5.60422	2.63253	0.17446
C	-6.72893	-0.35857	-0.75814
C	6.68179	0.82270	-0.95194
C	-5.47511	0.23552	-0.73314
C	5.51587	0.08016	-0.80509
N	-4.38990	-0.42875	-0.29671
N	4.42712	0.58670	-0.20012
O	-1.74333	0.83725	-2.05235
O	-3.42177	2.49063	-0.24718
O	2.15059	-1.13353	-1.83889
O	4.13302	-2.09571	0.82839
O	-1.63077	-1.40899	-0.41156
O	-2.26592	0.14008	1.94012
O	1.70573	1.25287	-0.58058
O	2.49943	0.23230	2.03002
O	0.37994	-1.06098	0.46780
O	-4.33389	0.95697	2.40253
O	-0.37194	1.49576	0.25175
O	1.99314	-1.73954	3.01069
O	-3.80149	0.95053	-3.01375
O	-2.43774	3.35833	1.60254
O	4.09705	-2.21523	-2.29687
O	2.32108	-3.19179	0.21879
Pb	-2.36324	0.70340	-0.04885
Pb	2.50518	-0.74470	0.19435
H	-8.30505	-3.15288	0.38365
H	-3.61844	-2.17861	0.48569
H	3.56851	2.19874	0.76699
H	-5.80651	-3.36709	0.49562
H	5.58983	3.63948	0.57947
H	-7.57692	0.21582	-1.11667
H	7.53240	0.37496	-1.45589
H	-5.30917	1.24887	-1.07171
H	5.42155	-0.93111	-1.18566
C	8.00765	2.95073	-0.56708
H	8.63102	2.61792	-1.40090
H	7.77986	4.01158	-0.70382
H	8.60448	2.86018	0.34865
H	-9.04697	-1.64790	-0.19685
H	-8.39702	-2.81723	-1.34829
H	4.00957	-4.12472	0.89248
H	2.17375	0.03772	3.99569
H	-0.10267	-2.70914	-0.63471
H	-3.85630	4.30113	0.48406
H	-2.03309	1.03410	-4.01290
H	0.37392	2.54293	-1.32709
H	2.51031	-2.06933	-3.55854
H	-3.04841	0.16706	3.77352

TGA Analysis

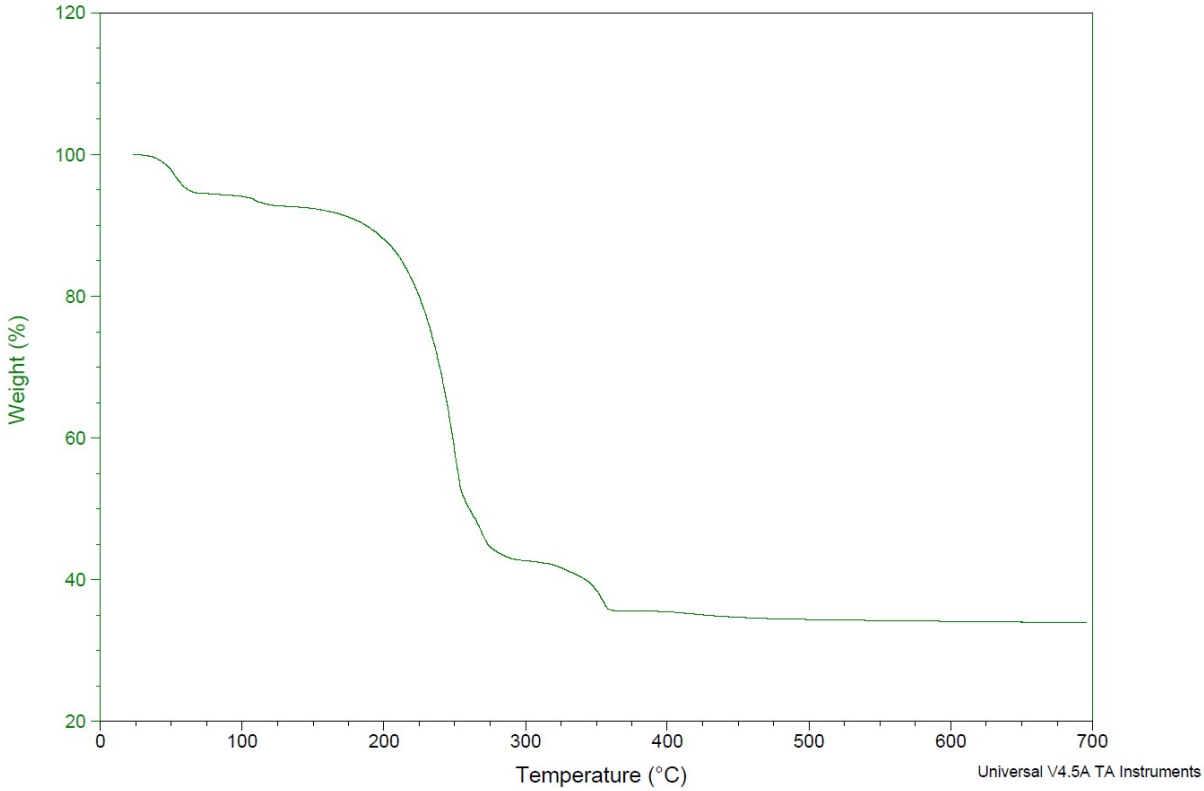

Figure S18. TGA analysis of **1**.

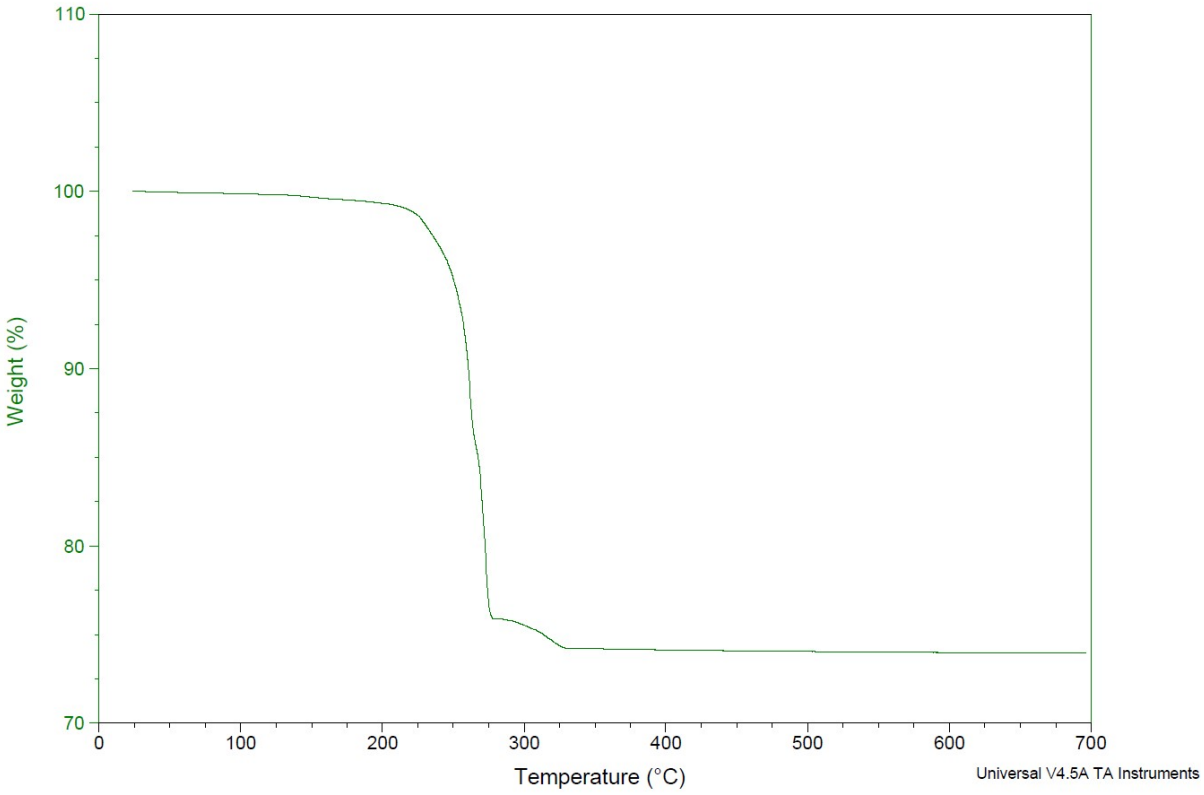

Figure S19. TGA analysis of **2**.

.